

Study of nonlinear optical characteristics of various media by the methods of z -scan and third harmonic generation of laser radiation

R.A. Ganeev, N.V. Kamanina, I.A. Kulagin, A.I. Ryasnyansky, R.I. Tugushev, T. Usmanov

Abstract. The nonlinear optical parameters of colloidal solutions of metals, semiconductor chalcogenide films, vapours and solutions of organic dyes, as well as of fullerene-doped polyimide films are studied by the methods of z -scan and third harmonic generation (THG). The nonlinear refractive indices, nonlinear susceptibilities, and nonlinear absorption coefficients of these materials are measured at the fundamental 1064-nm emission wavelength of a 35-ps pulsed Nd:YAG laser and its second harmonic at 532 nm. The study of the optical limitation of picosecond and nanosecond light pulses in these media showed that the appearance of the long-wavelength absorption band at the final stage of aggregation of colloidal metals resulted in nonlinear absorption of picosecond pulses. The nonlinear susceptibilities $\chi^{(3)}(-3\omega, \omega, \omega, \omega)$ of colloidal metals, fullerenes, and dye vapours are measured by the picosecond THG method, and the effect of self-action on THG in these media is analysed.

Keywords: nonlinear optical refraction, nonlinear optical absorption, nonlinear susceptibilities.

1. Introduction

The study of nonlinear optical processes of self-focusing and self-defocusing in materials is of great scientific and applied interest. Materials with high optical nonlinearities are promising for the use in optical limiters, optical switchers, etc. The study of optical limitation (OL) in various materials opens up new possibilities of their application in laser systems to control the parameters of the latter and to protect them from intense laser radiation. The OL mechanisms can be different. The OL in colloidal metals [1], fullerenes and phthalocyanines [2] occurs due to reverse saturated absorption, which is caused by a high

cross section for absorption from excited levels. The OL in inorganic clusters [3] is caused by intense nonlinear refraction, while in semiconductors, it is due to two-photon absorption [4].

In earlier experimental studies of nonlinear optical properties of media, a highly sensitive single-beam z -scan method was used for measuring the nonlinear refractive index, nonlinear susceptibility, and nonlinear absorption coefficient [4, 5]. In this method, a change in the intensity profile of a Gaussian beam in the far-field zone is studied by moving a sample along the longitudinal z axis in the focusing region. Another method for studying nonlinear optical properties of media is a conversion of the laser radiation frequency. The investigations of the second and third harmonic generation (THG) are one of the main methods used for measuring nonlinear optical susceptibilities of materials.

In this paper, we used the methods of z -scan and THG for studying nonlinear optical parameters of colloidal solutions of metals (silver, gold, platinum, copper), chalcogenide films (As_2S_3 , $\text{As}_{20}\text{S}_{80}$, $2\text{As}_2\text{S}_3/\text{As}_2\text{Se}_3$, $3\text{As}_2\text{S}_3/\text{As}_2\text{Se}_3$), vapours and solutions of organic dyes (naphthalene, paraterphenyl, anthracene, pentacene, and tetracene), and fullerene (C_{60} and C_{70}) films and solutions.

2. Basic equations

We analyse the nonlinear optical response of media within the framework of the perturbation theory [6]. The third-order nonlinear susceptibility $\chi_m^{(3)}(-3\omega, \omega, \omega, \omega) = \chi^{(3)}(-3\omega, \omega, \omega, \omega)/N$ (where N is the concentration of a substance), which is responsible for harmonic generation, was calculated from the known expression

$$\begin{aligned} \chi_m^{(3)}(-3\omega, \omega, \omega, \omega) = & \hbar^{-3} \sum_{ijk} d_{gi} d_{ij} d_{jk} d_{kg} \{ (\omega_{ig} - \omega)^{-1} \\ & \times (\omega_{jg} - 2\omega)^{-1} [(\omega_{kg} - 3\omega)^{-1} + (\omega_{kg} + \omega)^{-1}] \\ & + (\omega_{jg} + 2\omega)^{-1} [(\omega_{ig} - \omega)^{-1} - (\omega_{kg} + \omega)^{-1}] \\ & + (\omega_{ig} + 2\omega)^{-1} (\omega_{kg} + 3\omega)^{-1} \}, \end{aligned} \quad (1)$$

where ω_{gi} and d_{gi} are the frequency and matrix element of the operator of the dipole transition moment and ω is the frequency of fundamental radiation.

R.A. Ganeev, I.A. Kulagin, R.I. Tugushev, T. Usmanov 'Akademprigor' Research and Device Enterprise, Academy of Sciences of Uzbekistan, Akademgorodok, 700125 Tashkent, Uzbekistan; e-mail: rganeev@mail.tps.uz;

N.V. Kamanina Institute of Laser Physics, Birzhevaya lin. 12, 199034 St. Petersburg, Russia;

A.I. Ryasnyansky A. Navoi Samarkand State University, 703004, Uzbekistan

Received 19 March 2002; revision received 19 July 2002

Kvantovaya Elektronika 32 (9) 781–788 (2002)

Translated by M.N. Sapozhnikov

The third-order nonlinear susceptibilities $[\chi_k^{(3)}(-\omega, \omega, -\omega, \omega) = \chi^{(3)}(-\omega, \omega, -\omega, \omega)/N]$ responsible for the Kerr effect were calculated from the expression [7, 8]

$$\begin{aligned} \chi_k^{(3)}(-\omega, \omega, -\omega, \omega) \\ = \hbar^{-3} \sum_{ijk} d_{gi} d_{ij} d_{jk} d_{kg} (C_{gi,gi,gk} - C_{ig,jg,kg}). \end{aligned} \quad (2)$$

Here,

$$\begin{aligned} C_{gi,gi,gk} &= [(\omega_{kg} - \omega)^{-1} + (\omega_{kg} + \omega)^{-1}] (\omega_{ig} - \omega)^{-1} \\ &\times (\omega_{jg} - 2\omega)^{-1} \pm (1 - \delta_{gi}) [(\omega_{kg} - \omega)^{-1} + (\omega_{kg} + \omega)^{-1}] \\ &\times \omega_{jg}^{-1} (\omega_{jg} \pm \omega)^{-1} + \delta_{gj} [(\omega_{kg} - \omega)^{-1} + (\omega_{kg} + \omega)^{-1}] (\omega_{ij} \pm \omega)^{-2}. \end{aligned}$$

The experimental values of the refractive index n_2 were determined from standard equations of the z -scan theory. The normalised difference ΔT_{pv} of the maximum and minimum transmissions and the nonlinear phase shift $\Delta\Phi_0$ are related with n_2 by the expressions [4]

$$\Delta T_{pv} = 0.404(1 - S)^{0.25} |\Delta\Phi_0|, \quad (3)$$

$$\Delta\Phi_0 = \frac{2\pi}{\lambda} n_2 I_0 L_{\text{eff}}, \quad (4)$$

where I_0 is the maximum radiation intensity on the z axis; S is the transmission of an aperture in the limiting-aperture z -scan scheme; $L_{\text{eff}} = [1 - \exp(-\alpha L)]/\alpha$ is the effective length of a sample; α is the linear absorption coefficient; and L is the medium length.

The nonlinear absorption coefficient β was determined from equations describing the normalised transmission in the open-aperture z -scan scheme:

$$T_0 = q_0^{-1} \ln(1 + q_0), \quad (5)$$

$$q_0(0) = q_0 = \beta I_0 L_{\text{eff}}, \quad (6)$$

where T_0 and q_0 are the minimum of the normalised transmission in the open-aperture scheme and a dimensionless parameter, respectively.

Analysis of the limiting-aperture z -scheme was used for studying OL [4]. The position of a sample corresponded to the minimum transmission (in front of the focus upon self-focusing, and behind the focus upon self-defocusing), when the influence of two-photon absorption and inverse absorption saturation was negligible. In this case, the minimum transmission T_v is proportional to the laser radiation intensity and the third-order nonlinear susceptibility:

$$T_v = B I_0 \chi^{(3)}(-\omega, \omega, -\omega, \omega), \quad (7)$$

where B is a parameter independent of the radiation intensity.

A nonlinear response of media was also analysed by studying frequency conversion of laser radiation. The study of generation of harmonics made it possible to measure nonlinear susceptibilities responsible for this process and take into account the effect of Kerr nonlinearities [9]. In the case of weak focusing of fundamental radiation (the length L of the medium is much shorter than the confocal parameter b of the beam), we used the expression

$$I_{3\omega} = \gamma^2 L^2 I_{10}^3 \exp\left(-6k_1 \frac{r^2}{b}\right) \frac{\sin^2 \Delta(L, r)}{\Delta^2(L, r)} \quad (8)$$

for the third-harmonic intensity. Here, $\gamma = 24\pi^3 \chi^{(3)}(-3\omega, \omega, \omega, \omega)/(n_1^{3/2} n_3^{1/2} c \lambda_1)$; $\Delta(L, r) = 2L/b - \rho - \varphi$; $\rho = L\Delta k/2$ is the normalised phase mismatch; r is the polar coordinate: $\varphi = 72\pi L \Delta \chi_k I_{10} \exp(-2k_1 r^2/b)$; $\Delta k = 3k_1 - k_3$; $\Delta \chi_k = \chi^{(3)}(-\omega, \omega, -\omega, \omega)/2 - n_1 \chi^{(3)}(-\omega, 3\omega, -3\omega, \omega)/n_3$ is the difference of Kerr nonlinearities responsible for a change in the refractive index at the fundamental and harmonic frequencies in the fundamental radiation field; λ_i , k_i and n_i are the wavelength, the wave number, and the refractive index at the i th radiation frequency; and I_{10} is the maximum intensity of radiation being converted in the waist plane. Expression (8) was used for calculating $\chi^{(3)}(-3\omega, \omega, \omega, \omega)$.

The study of effects related to the modulation of the refractive index of a medium upon conversion of the laser radiation frequency is both of scientific and practical interest. On the one hand, this process restricts the harmonic conversion efficiency, but on the other it allows one to use new methods for efficient harmonic generation. In particular, in the case of tight focusing in gas media, the high-frequency Kerr effect changed the conditions of optimal phase matching and slowed down an increase in the third-harmonic intensity with increasing pump intensity [6].

An opposite situation is also possible, when the frequency conversion efficiency in media with a certain relation between linear and nonlinear phase mismatch increases due to the influence of a nonlinear phase mismatch [10]. Note that there is another possibility of generating harmonics by using higher order nonlinearities. In this case, at low concentrations of a substance, the harmonic intensity should be proportional to the square of concentration. On the other hand, if a harmonic is generated due to Kerr nonlinearities, its intensity should be proportional to the fourth power of concentration.

3. Experimental

We used a picosecond Nd:YAG laser in experiments. A single 35-ps laser pulse was amplified up to 2.4 mJ. We studied the nonlinear optical parameters of samples at the fundamental radiation wavelength 1064 nm and at the second-harmonic wavelength 532 nm. SHG was performed in a KDP crystal. Laser radiation was focused by a lens with a focal length of 25 cm. Samples (5-mm thick quartz cells with solutions or films of polyimide doped with fullerenes and semiconductor films) were mounted on a translation stage providing ultra-precision motion along the z axis through the focal plane with a resolution of 1 μm . The size of a focused laser spot at the beam waist was 150

and 100 μm for 1064 and 532 nm, respectively. The maximum radiation intensity of the fundamental and second harmonics was 4×10^{11} and $8 \times 10^{10} \text{ W cm}^{-2}$, respectively.

The laser pulse energy was measured with a calibrated FD-24K photodiode and recorded with a digital V4-17 voltmeter by using calibrated neutral filters. An aperture of diameter 1 mm was placed at a distance of 150 cm from the focal plane (the so-called limiting-aperture scheme), which transmitted $\sim 3\%$ of laser radiation. Behind the aperture, an FD-24K photodiode was placed, whose output signal was fed to a digital V4-17 voltmeter. To eliminate the effect of the laser output instability on the results of measurements, the intensity of radiation propagated through the aperture was normalised to the signal detected by the first photodiode. Each point on the experimental plots presented below was averaged over 20 pulses.

The limiting-aperture scheme allows one to determine the sign and value of n_2 for solutions and films, as well as their nonlinear susceptibilities $\chi^{(3)}$. To measure the coefficient β , the aperture was removed and the dependence of the transmission of solutions and films on their position with respect to the focal point of radiation was measured (the so-called open-aperture scheme). The dependence of the transmission of samples on the laser beam intensity was measured with a detector with a sufficiently large aperture located at a distance from the focal point that provided the detection of all radiation transmitted by samples. Thus, by measuring variations in the transmission of samples in the open-aperture scheme, we determined the nonlinear absorption coefficient.

A Q -switched 1064-nm, 28-ns, 18-mJ Nd:YAG laser was used as a source of nanosecond pulses. The maximum intensity of radiation focused with a lens with a focal length of 20 cm was $8 \times 10^9 \text{ W cm}^{-2}$ (the beam waist diameter was 100 μm). The time parameters of nanosecond radiation transmitted through a cell and aperture were measured with a coaxial photomultiplier and an oscilloscope. The size of silver and gold aggregates was measured with an electron microscope.

In THG experiments, radiation was focused on samples with a lens with a focal length of 25 cm. The pump radiation was detected with a calibrated FD-24K photodiode and a digital V4-17 voltmeter. The converted radiation at 354.7 nm was separated with an UFS-2 filter from pump radiation and directed to a diffraction DFS-452 spectrograph equipped with a FEU-106 photomultiplier, whose output signal was fed to a digital V4-17 voltmeter. The absolute values of the conversion efficiency were calibrated by converting laser radiation to the second and third harmonics in KDP crystals. The third-harmonic energy transmitted through a cell was measured with a calorimeter. Then, this radiation was appropriately attenuated with the help of calibrated filters. The calibration coefficient relating the third-harmonic energy to the output signal from the photomultiplier was determined using the aperture ratio of the spectrograph.

Colloidal solutions were prepared in the following way. Colloidal gold was prepared by adding 15 ml of 1% sodium citrate solution to 300 ml of heated HAuCl_4 solution (35 mg of salt in twice-distilled water). Then, the solution was evaporated to 1/3 of its initial volume, cooled to room temperature and filtered. A standard colloidal solution was prepared from platinum. 0.1 g of platinum was dissolved

upon heating in a few millilitres of a mixture of nitric and sulphuric acids and evaporated. Then, 5 ml of concentrated sulphuric acid and 0.1 g of sodium chloride were added and again evaporated. A dry residue was dissolved in 20 ml of diluted (1:1) sulphuric acid. 1 ml of a solution obtained in this way contained 1 mg of platinum.

A standard solution of colloidal copper was prepared by dissolving 4 g of CuSO_4 in one litre of distilled water. In this case, 1 ml of the solution contained 1 mg of copper. A standard solution of silver was prepared by dissolving 20 mg of collargol in 200 ml of twice-distilled water. Then, the solution was heated until it become yellow. The size of metal clusters depended on the aggregation degree and, according to the electron microscope analysis, was from 10 to 60 nm.

We studied 1- μm thick polyimide films doped with fullerene C_{70} and solutions of C_{60} and C_{70} in toluene. The weight concentration of C_{70} in the films was 0.2% and 0.5%; the concentration of C_{60} in solutions was 0.05% and 0.5%, and the concentration of C_{70} was 0.1% and 1%.

We also studied 10- μm thick semiconductor films of As_2S_3 , $\text{As}_{20}\text{S}_{80}$, $2\text{As}_2\text{S}_3/\text{As}_2\text{Se}_3$, and $3\text{As}_2\text{S}_3/\text{As}_2\text{Se}_3$. The radiation wavelengths 1064 or 532 nm corresponded to the energy range $E_g/2 < \hbar\omega < E_g$, where E_g is the energy gap and $\hbar\omega$ is the laser photon energy.

Solutions of paraterphenyl and naphthalene in toluene were used for studying Kerr nonlinear susceptibility.

4. Kerr nonlinear susceptibilities and nonlinear refraction coefficients of colloidal metal solutions, fullerenes, and organic dyes

We present below the results of the study of colloidal solutions of metals at the initial stage of aggregation. Fig. 1a shows the typical dependences of the normalised transmission T of samples in the limiting-aperture scheme on the position of a cell containing the solution of colloidal gold with respect to the focal point in the field of picosecond 1064-nm and 532-nm pulses. Similar dependences were obtained for other colloidal solutions. Except the gold solution, all colloidal solutions had positive nonlinear refraction indices. The nonlinearity signs did not change at a wavelength of 532 nm as well, except the copper solution, where the nonlinear refractive index changes its sign from positive to negative. These dependences are caused by the influence of Kerr nonlinearities in the field of strong electromagnetic radiation.

In picosecond experiments, we chose the radiation intensity at the focus so that to avoid an optical breakdown on the cell surface and inside it. For example, for the solution of colloidal gold, the intensity $I \leq 4 \times 10^{11} \text{ W cm}^{-2}$ was used, which was below the optical breakdown threshold equal to $8 \times 10^{11} \text{ W cm}^{-2}$ (at 1064 nm). We calculated the nonlinear optical parameters of colloidal metals from expressions (3) and (4). In particular, the nonlinear refractive index n_2 of colloidal gold proved to be equal to -1.82×10^{-14} esu at 1064 nm and -1.96×10^{-13} esu at 532 nm. The nonlinear susceptibility was $\chi^{(3)}(-\omega, \omega, -\omega, \omega)$ was equal to -2.5×10^{-15} and -2.7×10^{-14} esu at wavelengths 1064 and 532 nm, respectively. The latter value is in good agreement with the value of $\chi^{(3)}$ obtained in paper [11]. The nonlinear susceptibilities for Ag, Pt, and Cu solutions were determined in a similar way. The values of the nonlinear refractive index and nonlinear susceptibility measured at two wavelengths are presented in Table 1.

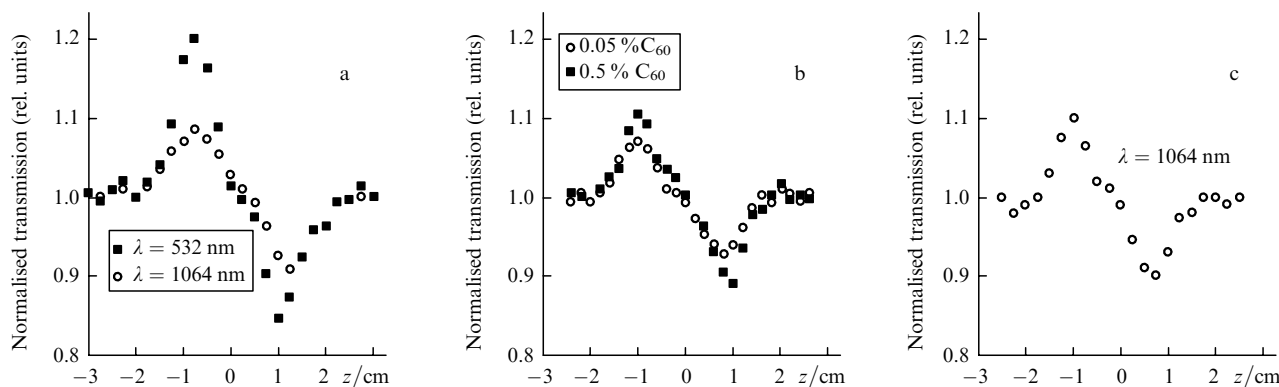


Figure 1. Dependences of the normalised transmission on the position of samples in the limiting-aperture scheme for colloidal gold (a), fullerene (b) and paraterphenyl (c) solutions in toluene.

Table 1. Nonlinear refractive indices and nonlinear susceptibilities of colloidal metals.

Metal	$n_2/10^{-14}$ esu		$\chi^{(3)}(-\omega, \omega, \omega, \omega)/10^{-15}$ esu	
	$\lambda = 1064$ nm	$\lambda = 532$ nm	$\lambda = 1064$ nm	$\lambda = 532$ nm
Au	-1.82	-19.6	-2.51	-27
Ag	3.4	10.2	4.7	14
Cu	4.2	-13.8	5.8	-19
Pt	1.13	8.8	1.56	12.1

The nonlinear optical parameters of colloidal metals were also studied in the field of nanosecond pulses. We obtained the values of $\chi^{(3)} = 1.5 \times 10^{-12}$, 3.3×10^{-12} and 2.4×10^{-12} esu at 1064 nm for Ag, Pt, and Cu, respectively. These values are two-three orders of magnitude greater than similar values observed upon excitation by picosecond pulses. In the case of nanosecond pulses, the temporal profile of a laser pulse changed after its propagation through a sample and an aperture [12]. This circumstance suggests the thermal nature of nonlinearity. The low nonlinear susceptibilities of samples can be explained by the fact that we used non-aggregated solutions in this series of experiments. The dependence of nonlinear optical parameters of colloidal solutions on the degree of their aggregation was analysed in paper [12].

Fig. 1b shows the dependences of the transmission of a cell with C_{60} solutions in toluene on the position of the cell with respect to the focal point for the fundamental and second-harmonic wavelengths of a picosecond laser. Similar dependences were also obtained for C_{70} solutions and films.

Table 2. Nonlinear optical characteristics of fullerene films and solutions at a wavelength of 1064 nm.

Medium	$n_2/10^{-11}$ esu	$\chi^{(3)}(-\omega, \omega, \omega, \omega)/10^{-12}$ esu
Polyimide film containing 0.2 % of C_{70}	-120	-166
Polyimide film containing 0.5 % of C_{70}	-140	-223
0.1 % solution of C_{70} in toluene	-0.05	-0.069
0.5% solution of C_{60} in toluene	-0.13	-0.18

One can see that the nonlinear refractive index for all the samples is negative. For the 0.5 % solution of C_{60} in toluene, $n_2 = -1.3 \times 10^{-12}$ esu and the parameter $\chi^{(3)} = -1.8 \times 10^{-13}$ esu at 1064 nm. We found nonlinear absorption only for the C_{60} solution. We will analyse the mechanism of nonlinear absorption in more detail in Section 5. Table 2 presents the values of the nonlinear refractive index and nonlinear susceptibility of fullerene films and solutions obtained at 1064 nm.

We present below the results of the study of the third-order nonlinear susceptibility and nonlinear refractive index for a number of organic dyes (naphthalene, paraterphenyl, anthracene, pentacene, and tetracene). The third-order Kerr susceptibility of a single molecule was calculated from expressions (1) and (2). The values of $\chi_k^{(3)}$ and n_2/N calculated for different organic dyes are presented in Table 3. We measured the values of $\chi^{(3)}(-\omega, \omega, -\omega, \omega)$ and n_2 for the solution of paraterphenyl in toluene by the z -scan method and compared them with theoretical calculations. Fig. 1c shows the typical dependence $T(z)$ for the solution of paraterphenyl in toluene. We calculated the nonlinear optical characteristics $\chi^{(3)}(-\omega, \omega, -\omega, \omega)$ and n_2 for paraterphenyl [$\chi^{(3)}(-\omega, \omega, -\omega, \omega) = n_2 \times n_0/3\pi$; where n_0 is the linear refractive index] from expressions (3) and (4). The nonlinear susceptibility $\chi_k^{(3)}(-\omega, \omega, -\omega, \omega)$ and nonlinear refractive index n_2 of paraterphenyl were found to be $(-1 \pm 0.5) \times 10^{-30}$ and $(-3 \pm 1.5) \times 10^{-10}$ esu, respectively, at the concentration $N = 5 \times 10^{19} \text{ cm}^{-3}$.

Table 3. Kerr nonlinearities and nonlinear refractive indices of organic dyes at a wavelength of 1064 nm.

Organic dye	$\chi_k^{(3)}(-\omega, \omega, \omega, \omega)/\text{esu}$	$n_2/N/\text{esu}$
Naphthalene	1.54×10^{-33}	9×10^{-33}
Anthracene	1.08×10^{-31}	6×10^{-31}
Tetracene	5×10^{-29}	3×10^{-28}
Pentacene	-2.46×10^{-29}	-1.5×10^{-28}
Paraterphenyl	-4.15×10^{-30}	-2.5×10^{-29}

A comparison of the experimental and theoretical values of the Kerr nonlinear susceptibility and nonlinear refractive index of organic dyes studied showed their satisfactory agreement. The difference between the experimental values and the values calculated with the help of the free electron

model can be caused both by an error in the calculation of dipole moments and the influence of a solvent on the experimental results.

Our calculations showed that some of the molecules (tetracene, paraterphenyl, pentacene) had strong Kerr nonlinearities, which can substantially affect the process of frequency conversion in these media. In this case, a strong violation of the phase matching between the pump and harmonic waves can be observed, caused by a change in the refractive index at these frequencies induced by high-power laser radiation. The consideration of this factor allows us to calculate the optimal conditions of the phase mismatch between the interacting waves upon frequency conversion of laser radiation in organic dyes.

As mentioned above, media possessing high Kerr nonlinearities can be used as optical limiters. In this connection, of interest is the nonlinear refractive index $n_2 = -7.5 \times 10^{-9}$ esu we obtained for pentacene at the concentration $N = 5 \times 10^{19} \text{ cm}^{-3}$. In a certain combination with other materials, this medium, which produces strong defocusing, can be used as an efficient optical limiter.

5. Optical limitation in fullerenes, colloidal metals, and semiconductors

Most optical-limitation studies of fullerenes C_{60} and C_{70} were earlier performed using 532-nm nanosecond pulses [2]. We present below the experimental results on optical limitation upon excitation of fullerenes by picosecond pulses at 1064 and 532 nm. Fig. 2a shows the dependence of the normalised transmission on the laser radiation intensity at 1064 nm. We observed optical limitation only in the solution of C_{60} , whereas no noticeable change in the transmission of laser radiation at 1064 nm was observed in the C_{70} solution. Fig. 2a shows also similar dependences for solutions of C_{60} and C_{70} for a wavelength of 532 nm. In this case, optical limitation was observed for all the samples studied.

The study of the concentration dependences showed a linear increase of optical limitation with increasing fullerene concentration. For the 0.5% solution of C_{60} , the nonlinear absorption coefficient at 1064 nm was $1.5 \times 10^{-10} \text{ cm W}^{-1}$. The absence of a noticeable nonlinear absorption in films and solutions of C_{70} is explained by the fact that the resonance lines of C_{70} lie in the UV region, which reduces the probability of two-photon absorption at 1064 nm. In the case of C_{60} , the resonance line is located at 565 nm, providing the possibility of two-photon absorption. The nonlinear absorption coefficients were $2.2 \times 10^{-10} \text{ cm W}^{-1}$ for the 0.5% solution of C_{60} at 532 nm and $4.5 \times 10^{-11} \text{ cm W}^{-1}$ for the 0.1% solution of C_{70} at 532 nm.

Our study showed that nonlinear absorption is caused by reverse saturated absorption (due to a stronger absorption from the excited state than from the ground state) at 532 nm, as well as by a combined action of two-photon absorption and reverse saturated absorption at 1064 nm in the solution of C_{60} [13].

Optical limitation in colloidal metal structures was studied earlier using the 532-nm second harmonic of a Nd:YAG laser [11]. Below, we present the results of the study of optical limitation in colloidal metals at 1064 nm using both picosecond and nanosecond pulses. Picosecond pulses were used to study aggregated solutions of gold and silver. As mentioned above, the optical and nonlinear

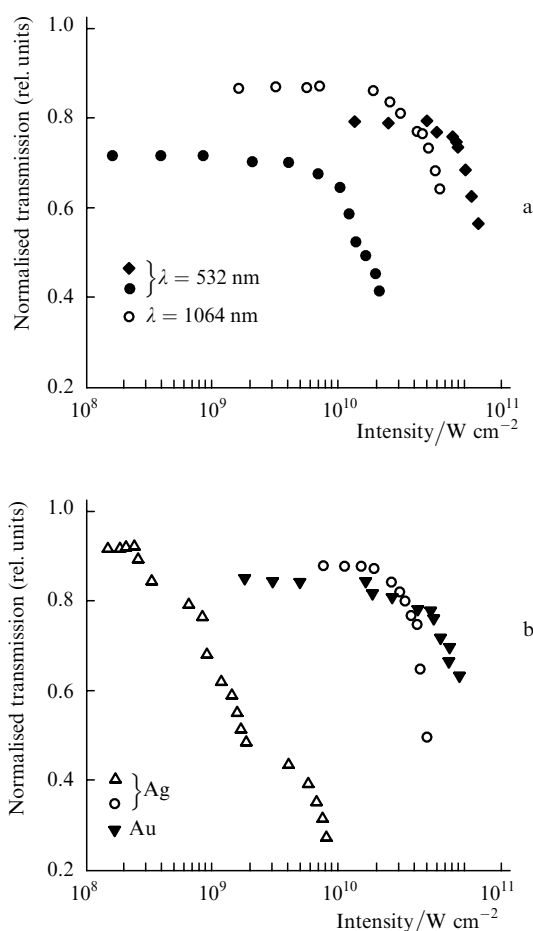


Figure 2. Dependences of the normalised transmission of 0.5% solution of fullerene C_{60} (○), 0.05% solution of C_{60} (●), and 0.1% solution of C_{70} (◆) irradiated by picosecond pulses (a) and of solutions of colloidal metals irradiated by picosecond (▼,○) and nanosecond (△) pulses (b).

optical properties of aggregated solutions are determined by the dynamics of the absorption spectrum. The dependences of the normalised transmission on the radiation intensity for aggregated silver and gold are presented in Fig. 2b. Note that solutions did not exhibit optical limitation at the initial stage of aggregation.

Our study of nonlinear absorption using the open-aperture z-scheme showed that it appeared only at the final stage of aggregation. Plasmon resonance peaks in aggregated solutions were located at 565 nm for gold and at 580 nm for silver, whereas the peaks in non-aggregated solutions were located at 525 and 415 nm, respectively. The nonlinear absorption coefficients β for colloidal gold were $9.8 \times 10^{-13} \text{ cm W}^{-1}$ at 1064 nm and $9.4 \times 10^{-12} \text{ cm W}^{-1}$ at 532 nm. In the case of nanosecond pulses, optical limitation was observed both in aggregated and non-aggregated solutions. The dynamics of this process in different aggregate states of colloidal silver was studied using picosecond and nanosecond pulses in paper [12].

We found that the nonlinear refractive index of some chalcogenide films was rather high. For example, $n_2 = 1.3 \times 10^{-8}$ esu at 532 nm for As_2Se_3 . The greatest value of n_2 equal to -2.6×10^{-8} esu at 1064 nm was observed for the $2As_2S_3/As_2Se_3$ film. The values of n_2 were measured using the experimental parameters ΔT_{p1} , α , L , and the linear refractive index of chalcogenide films.

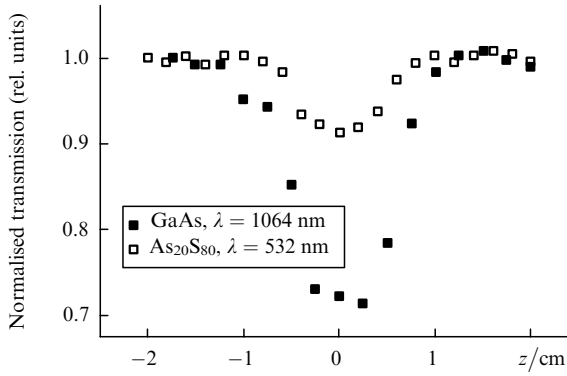


Figure 3. Dependences of the normalised transmission of a GaAs plate and $\text{As}_{20}\text{S}_{80}$ chalcogenide films at wavelengths of 1064 and 532 nm on their position in the open-aperture scheme.

We found two-photon absorption in all semiconductor films studied. Fig. 3 shows the dependences of the normalised transmission on the position of the $\text{As}_{20}\text{S}_{80}$ film obtained in the open-aperture scheme. For comparison, we also present here a similar dependence for a 0.4-mm thick GaAs plate obtained at the laser power density at the focal point equal to $1.3 \times 10^9 \text{ W cm}^{-2}$. At such a high power density, absorption was mainly determined by nonlinear absorption. Linear absorption in chalcogenide films under study was very weak. For example, the linear absorption coefficient of the As_2S_3 film was 0.095 cm^{-1} at 1064 nm.

The nonlinear absorption coefficient β of the GaAs plate was $31 \times 10^{-9} \text{ cm W}^{-1}$, in good agreement with the value $26 \times 10^{-9} \text{ cm W}^{-1}$ measured earlier [14]. We found that the values of β for chalcogenide $\text{As}_{20}\text{S}_{80}$ ($\beta = 3 \times 10^{-6} \text{ cm W}^{-1}$ at 532 nm, $I_0 = 4 \times 10^8 \text{ W cm}^{-2}$) and $3\text{As}_2\text{S}_3/\text{As}_2\text{Se}_3$ ($\beta = 10^{-7} \text{ cm W}^{-1}$ at 1064 nm, $I_0 = 7 \times 10^8 \text{ W cm}^{-2}$) films were greater than that for the GaAs plate.

We studied optical limitation in semiconductors by using the open-aperture scheme, as in the study of nonlinear absorption. The sample position corresponded to the minimal transmission, i.e., the sample was located at the focal point. Optical limitation in this case was caused by two-photon absorption. The greatest limitation (by a factor of 25) was observed in As_2S_3 . As mentioned above, two-photon absorption in semiconductors is accompanied by the appearance of free carriers, which also contribute to the nonlinear character of propagation of radiation in these media. This effect was used in semiconductors GaAs, GaP, and CdSe applied as passive elements in generators of extended pulse trains with a passive negative feedback [15, 16]. The latter ones are not only very simple to realise, but also can generate compressed picosecond pulses with stable energy and temporal parameters, which are necessary for nonlinear-optical studies. Our study showed that the chalcogenide $2\text{As}_2\text{S}_3/\text{As}_2\text{Se}_3$ and $3\text{As}_2\text{S}_3/\text{As}_2\text{Se}_3$ films are promising for applications in such intracavity elements for compression of picosecond laser pulses.

6. Conversion of laser radiation frequency in organic dyes, fullerenes, and colloidal metals

We used organic dyes (naphthalene, anthracene, tetracene, pentacene, and paraterphenyl) as nonlinear media for

studying THG. The number of conjugated bonds in the first four molecules is $j = 5, 7, 9,$ and $11,$ respectively. We calculated the nonlinear susceptibilities of organic dyes using the free electron model. The value of the nonlinear susceptibility for naphthalene proved to be $\chi_m^{(3)}(-3\omega, \omega, \omega, \omega) = 0.42 \times 10^{-33} \text{ esu}$.

The THG can be realised in isotropic media, along with the direct ($\omega + \omega + \omega \rightarrow 3\omega$) process, by generating the difference frequency in the process ($\omega + \omega + \omega + \omega - \omega \rightarrow 3\omega$). We calculated for the latter case the fifth-order nonlinear susceptibility using the similar method. The fifth-order nonlinear $\chi_m^{(5)}(-3\omega, \omega, \omega, \omega, -\omega)$ susceptibility for naphthalene proved to be $1.3 \times 10^{-46} \text{ esu}$.

The third- and fifth-order nonlinear susceptibilities calculated for THG in vapours of organic dyes are presented in Table 4. Note that the values of $\chi_m^{(3)}$ for paraterphenyl and pentacene are rather large (2.35×10^{-30} and $1.66 \times 10^{-30} \text{ esu}$, respectively), being comparable with the nonlinearities of alkali metal atoms. Analysis of these results shows that nonlinear susceptibilities responsible for the harmonic generation substantially increase with increasing length L of conjugated bonds in molecules.

Table 4. Third- and fifth-order nonlinear susceptibilities responsible for THG in organic dyes at 1064 nm.

Organic dye	L/nm	$\chi_m^{(3)}(-3\omega, \omega, \omega, \omega)/\text{esu}$	$\chi_m^{(5)}(-3\omega, \omega, \omega, \omega, -\omega)/\text{esu}$
Naphthalene	0.7	0.42×10^{-34}	1.3×10^{-46}
Anthracene	0.98	2.8×10^{-33}	6×10^{-44}
Tetracene	1.26	7.4×10^{-31}	2.85×10^{-40}
Pentacene	1.54	1.66×10^{-30}	9.6×10^{-39}
Paraterphenyl	1.4	2.35×10^{-30}	7×10^{-38}

Consider now the main results of the study of THG in naphthalene vapour [17]. The maximum radiation conversion efficiency (10^{-8}) was observed at 170°C . It is most likely that THG in naphthalene occurs due to six-photon difference process $\omega + \omega + \omega + \omega - \omega \rightarrow 3\omega$. A similar generation of the difference frequency was observed earlier in naphthalene vapour due to the process $2\omega + 2\omega - \omega \rightarrow 3\omega$ [18]. Note that the generation of the difference frequency can occur both for positive and negative values of Δk , i.e., this process can be observed in media with normal and anomalous dispersion. The optimal conditions for this process are realised when $b\Delta k = -0.2$ (b is a confocal parameter). According to experimental data [17], $\chi_m^{(5)}(-3\omega, \omega, \omega, \omega, -\omega) = 10^{-48} \text{ esu}$.

Below, we present the results of the study of THG in polyimide films doped with fullerene C_{70} . Fig. 4 shows the dependence of the third-harmonic intensity on the fundamental pump radiation intensity for a film containing 0.5% of C_{70} . This dependence was described by a cubic law up to the pump intensity $I = 5 \times 10^{10} \text{ W cm}^{-2}$. As the pump intensity was further increased, a deviation from a cubic dependence was observed, which was predicted by the theory of generation of odd harmonics upon conversion of a wave with a plane phase front. Calculations based on the measured values showed that nonlinear refraction affects the fulfilment of phase matching during THG and is responsible for the deviation of the dependence $I_{3\omega}(I_\omega)$ from a cubic law (Fig. 4, solid curve). For a film containing

0.2% of C_{70} , the slope of the dependence $I_{3\omega}(I_\omega)$ was 2.8 over the entire interval of the pump intensity. The maximum conversion efficiencies for films containing 0.2% and 0.5% of C_{70} were 10^{-6} and 6×10^{-6} , respectively. No THG was observed in a pure polyimide film. The THG in films doped with fullerene C_{70} was described in detail in paper [19].

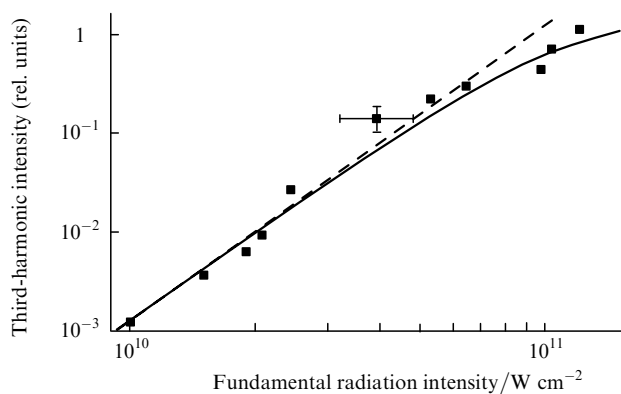


Figure 4. Cubic (dashed straight line) and experimental (solid curve) dependences of the third-harmonic intensity of the fundamental radiation intensity for polyimide films containing 0.5% of C_{70} .

We studied THG in colloidal films in order to determine the nonlinear susceptibility $\chi^{(3)}(-3\omega, \omega, \omega, \omega)$ in the UV region and to analyse the factors that restrict the frequency conversion efficiency. The slope of the dependence $I_{3\omega}(I_\omega)$ was 2.8 over the entire interval of the pump intensity, which is close to the theoretical result. The maximum THG efficiency for colloidal platinum and copper were 7×10^{-7} and 3×10^{-7} , respectively. The nonlinear susceptibilities of colloidal solutions of Pt and Cu under our experimental conditions were 2×10^{-14} and 10^{-14} esu, respectively.

We studied the influence of the quadratic Kerr effect on the phase characteristics of THG, taking into account the values of nonlinear refractive indices of solutions of Pt and Cu measured earlier. The theoretical analysis showed that, for a given radiation intensity, a nonlinear addition to the refractive index should not affect a cubic dependence $I_{3\omega}(I_\omega)$.

7. Conclusions

We have studied the nonlinear optical properties of colloidal solutions of metals (silver, gold, platinum, and copper), semiconductor chalcogenide films (As_2S_3 , $As_{20}S_{80}$, $2As_2S_3/As_2Se_3$, $3As_2S_3/As_2Se_3$), vapours and solutions of organic dyes (naphthalene, paraterphenyl, anthracene, pentacene, and tetracene), and fullerene (C_{60} and C_{70}) solutions and films by the methods of z-scan and THG. The measurements of nonlinear refractive indices, nonlinear susceptibilities and nonlinear absorption coefficients at the fundamental and second-harmonic wavelengths of a Nd:YAG laser have shown that colloidal solutions of Cu, Ag, and Pt have positive nonlinear refractive indices at 1064 nm, whereas the nonlinear refractive index of colloidal gold is negative. A similar situation was observed at a wavelength of 532 nm, except the Cu solution, in which the positive sign of the nonlinear refractive index changed to

the opposite. We have shown also that nonlinear absorption becomes noticeable at final aggregation stages resulting in the appearance of a long-wavelength wing in the absorption spectrum.

We have also studied optical limitation in fullerene solutions, colloidal metals, and semiconductor chalcogenide films and have shown that optical limitation can occur in the IR region in fullerene solutions excited by picosecond pulses. We also found that two-photon absorption affects optical limitation in semiconductor films.

We have investigated THG in colloidal metals, fullerene solutions, and organic dye vapours induced by a picosecond Nd:YAG laser. We have measured nonlinear susceptibilities $\chi^{(3)}(-3\omega, \omega, \omega, \omega)$ and considered the effect of self-action process on THG. We have found the effect of nonlinear refraction in fullerene films on phase matching conditions upon THG, which was manifested in the deviation of the dependence $I_{3\omega}(I_\omega)$ from a cubic law. We have also found that Kerr nonlinearities affect the phase matching conditions upon frequency conversion in anthracene and pentacene.

Acknowledgements. This work was partially supported by the Ukrainian Scientific and Technical Center (Project No. UZB-29).

References

1. Ji W., Du H.J., Tang S.H., Shi S. *J. Opt. Soc. Am. B*, **12**, 876 (1996).
2. Tutt L.W., Kost A. *Nature (London)*, **356**, 224 (1992).
3. Chen Z.R., Hou H.W., Xin X.Q., Yu K.B., Shi S. *J. Phys. Chem.*, **99**, 8717 (1995).
4. Sheik-Bahae M., Said A.A., Wei T., Hagan D.J., van Stryland E.W. *IEEE J. Quantum Electron.*, **26**, 760 (1990).
5. Sheik-Bahae M., Said A.A., Van Stryland E.W. *Opt. Lett.*, **14**, 955 (1989).
6. Reintjes J.F. *Nonlinear Optical Parametric Processes in Liquids and Gases* (New York: Academic Press, 1984).
7. Puell H., Vidal C.R. *Phys. Rev. A*, **14**, 2225 (1976).
8. Kulagin I.A., Usmanov T. *Kvantovaya Elektron.*, **30**, 520 (2000) [*Quantum Electron.*, **30**, 520 (2000)].
9. Kulagin I.A., Usmanov T. *Kvantovaya Elektron.*, **25**, 1121 (1998) [*Quantum Electron.*, **28**, 1089 (2000)].
10. Ganeev R.A., Kulagin I.A., Begishev I.A., Redkorechev V.I., Usmanov T. *Nonlinear Opt.*, **16**, 109 (1986).
11. Mehendale S.C., Mishra S.R., Bindra K.S., Laghate M., Dhama T.S., Rustagi K.S. *Opt. Commun.*, **133**, 273 (1997).
12. Ganeev R.A., Ryasnyansky A.I., Kodirov M.K., Kamalov S.R., Usmanov T. *J. Phys. D*, **34**, 1602 (2001).
13. Ganeev R.A., Ryasnyansky A.I., Kodirov M.K., Usmanov T. *Opt. Commun.*, **185**, 473 (2000).
14. Said A.A., Sheik-Bahae M., Hagan D.J., Wei T.H., Wang J., Van Stryland E.W. *J. Opt. Soc. Am. B*, **9**, 405 (1992).
15. Agnessi A., Del Corno A., Di Trapani P., Fogliani M., Reali G.P., Diels J.-C., Yen C.-Y., Zhao X.M., Kubecek V. *IEEE J. Quantum Electron.*, **28**, 710 (1992).

16. Ganeev R.A., Usmanov T. *Jpn J. Appl. Phys.*, **39**, 5111 (2000).
17. Ganeev R.A., Kamalov S.R., Kodirov M.K., Malikov M.R., Ryasnyansky A.I., Tugushev R.I., Umidullaev S.U., Usmanov T. *Opt. Commun.*, **184**, 305 (2000).
18. Aleksandrovsky A.S., Karpov S.V., Myslivets S.A., Popov A.K., Slabko V.V. *J. Phys. B*, **26**, 2965 (1993).
19. Ganeev R.A., Ryasnyansky A.I., Kamanina N.V., Kulagin I.A., Kodirov M.K., Usmanov T. *J. Opt. B*, **3**, 88 (2001).